Molecular Crystals and Liquid Crystals Science and Technology. Section A. Molecular Crystals and Liquid Crystals
Publication details, including instructions for authors and subscription information:
http://www.tandfonline.com/loi/gmcl19

Highly—Oriented BEDO-TTF Molecules in Metallic Polymer Composites

S. Hornchi [a], H. Yamochi [a], G. Saito [a], J. K. Jeszka [b], A. Tracz [b], A. Sroczynska [b] & J. Ulanski [c]

[a] Division of Chemistry, Graduate School of Science, Kyoto University, Sakyo-ku, Kyoto, 606-01, Japan

[b] Center of Molecular and Macromolecular Studies, Polish Academy of Sciences, ul. Sienkiewicza 112 90-363, Lodz, Poland

[c] Polymer Institute, Technical University of Lodz, Zwirki 36, 90-924, Lodz, Poland

Version of record first published: 24 Sep 2006

To cite this article: S. Hornchi, H. Yamochi, G. Saito, J. K. Jeszka, A. Tracz, A. Sroczynska & J. Ulanski (1997): Highly—Oriented BEDO-TTF Molecules in Metallic Polymer Composites, Molecular Crystals and Liquid Crystals Science and Technology. Section A. Molecular Crystals and Liquid Crystals, 296:1, 365-382

To link to this article: http://dx.doi.org/10.1080/10587259708032334

Mol. Cryst. Liq. Cryst., 1997, Vol. 296, pp. 365–382
Reprints available directly from the publisher
Photocopying permitted by license only

HIGHLY–ORIENTED BEDO–TTF MOLECULES IN METALLIC POLYMER COMPOSITES

SACHIO HORIUCHI,* HIDEKI YAMOCHI, and GUNZI SAITO*
Division of Chemistry, Graduate School of Science, Kyoto University, Sakyo-ku, Kyoto, 606–01, Japan

JEREMIASZ K. JESZKA, ADAM TRACZ, and AGNIESZKA SROCZYŃSKA,
Center of Molecular and Macromolecular Studies, Polish Academy of Sciences, ul. Sienkiewicza 112, 90–363 Lodz, Poland

JACEK ULAŃSKI
Polymer Institute, Technical University of Lodz, Zwirki 36, 90–924, Lodz, Poland

(Received 14 September 1996; In final form 16 October 1996)

Abstract Transport and optical properties of the metallic reticulate–doped polymer composites based on bis(ethylenedioxy)tetrathiafulvalene (BEDO–TTF) complexes are investigated, and compared with the structural and physical properties of the respective bulk crystals. Exposing the surface of polycarbonate (PC) film containing the molecularly dispersed donor to the solvent/(iodine or bromine) vapor converted the donor into charge–transfer (CT) complexes, which dominate the conducting and thermoelectric properties of the composites. Both film surfaces doped with bromine and iodine are well conducting, showing metallic behavior down to low temperatures. A characteristic CT band for the highly conducting states of the partially oxidized BEDO–TTF molecules appeared in the infrared region. However, compared with the respective bulk crystal, absorptions of the intramolecular excitation of the donor molecules are greatly diminished for the incident light perpendicular to the film surface. The PC film of (BEDO–TTF)–bromide exhibited high transparency for the visible light, in contrast with the film of (BEDO–TTF)–iodide which showed intense absorptions due to the intramolecular excitation of the I_3^- molecule in the visible region. Optical absorption spectra are anisotropic, which evidences the highly oriented BEDO–TTF molecules in the films. The molecular orientation was discussed in relation to the high conductivity and transparency. The crystal structure was also determined for newly obtained $(BEDO–TTF)_2Br(H_2O)_3$, the band structure calculation of which showed two–dimensional nature.

Keywords: reticulate–doped polymer composites, molecular metal, transparency, molecular orientation

INTRODUCTION

A number of molecular metals and superconductors have been developed mainly based on TTF analogues.[1-4] We have clarified that bis(ethylenedioxy)tetrathiafulvalene (BEDO–TTF) molecule is a particularly suitable component for molecular metals; both strong self-aggregation of the molecules and resulting two-dimensional (2D) electronic structure stabilize the metallic state to low temperatures, irrespectively to the nature of counter component molecules.[5-7] This novel property led to the formation of metallic network also in the Langmuir–Blodgett films of $(\text{BEDO–TTF})_5(\text{decyl–TCNQ})_2$[8,9] and $(\text{BEDO–TTF})_2(\text{2,5–dimethoxy–TCNQ})$.[10]

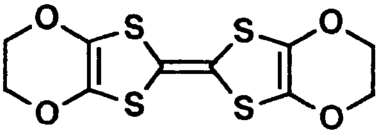

BEDO–TTF

Recently, the reticulate–doping technique, which was originally developed by Jeszka *et al.*,[11] has been applied to fabricate new metallic polymer composites of (BEDO–TTF)–iodide and (BEDO–TTF)–bromide complexes.[12,13] The reticulate–doping has provided various highly–conducting polymer composites, which have an extremely low percolation threshold and preserve mechanical properties of the matrix polymer.[14] Among them, $(\text{BEDT–TTF})_2I_3$–containing polycarbonate film (BEDT–TTF = bis(ethylenedithio)tetrathiafulvalene) was recently found to show metallic behavior and even (incomplete) superconductivity below 7 K after thermal treatment.[15] However, except for this BEDT-TTF salt, (BEDO–TTF)–iodide is the only example that yielded reticulate-doped composites with metallic character stabilized down to low temperatures (below 20 K). Besides, the other metallic film of (BEDO–TTF)–bromide exhibits high transparency, which is also one of the desired properties for the polymer composites.

In this paper, we present the optical and transport properties of the reticulate–doped polymer composites based on the above two BEDO–

TTF complexes. For comparison, we also give the corresponding properties of the bulk crystals. The electronic states and orientation of the donor molecules in the films are discussed in relation to the high conductivity and transparency.

EXPERIMENTAL

The synthesis and purification of BEDO–TTF were described elsewhere.[5] The $(BEDO–TTF)_{2.4}I_3$ ($\underline{1}$)[16] (greenish lustrous black elongated plates, decomposition point (*D*p) = 146–154 °C) was prepared by electrocrystallization of the donor in the presence of $[(n\text{–}C_4H_9)_4N]I_3$ in benzonitrile. The preparation of $(BEDO–TTF)I_3$ ($\underline{2}$) was described elsewhere.[17] The $(BEDO–TTF)_2Br(H_2O)_3$ ($\underline{3}$) crystals (black elongated plates, *D*p = 102–107 °C) were obtained either by electrochemical oxidation of BEDO–TTF in the presence of $[(C_2H_5)_4N]_2CoBr_4$ and water in benzonitrile or by direct reaction with bromine of 4:1 molar ratio in acetonitrile. The stoichiometries were determined by elementary analysis satisfactorily (± 0.3 % for C, H, O, S, Halogen).

The reticulate–doped polymer films of (BEDO–TTF)–iodide (or –bromide) (0.02–0.03 mm thickness) were prepared by the two–step method as described previously: (i) the poly(bisphenol–A–carbonate) (PC) films containing 1 wt% of molecularly–dispersed BEDO–TTF were made by casting the solution of the polymer and the donor, and (ii) the one side of each film was exposed to the vapor of CH_2Cl_2 containing 0.03 mol/l of iodine (or 2.5×10^{-6} mol/l of bromine).[18] The films treated with the vapor for 3 min, which were found to show the best metallic properties so far for both films, were used for the following measurements. The film without treatment (ii) was completely insulating, which prevented the measurements of its conductivity and thermoelectric power.

The structural data of $(BEDO–TTF)_2Br(H_2O)_3$ ($\underline{3}$) were obtained from a crystal of dimensions 0.35x0.18x0.06 mm^3 mounted on a four circle diffractometer (MAC Science MXC$^{\chi}$) equipped with a graphite monochrometer; Mo*K*α radiation. The space group is triclinic, $P\bar{1}$ with a = 5.3404(8) Å, b = 16.774(2) Å, c = 4.0226(6) Å, α = 87.85(1)°, β = 81.58(1)°, γ = 85.64(1)°, V = 355.30(8) Å^3, and Z = 1/2. No superlattices

TABLE I Atomic coordinates and Equivalent Isotropic Thermal Parameters in $(BEDO\text{-}TTF)_2Br(H_2O)_3$ (3).

Atom	x	y	z	B_{eq}
S1	-0.1230(2)	0.38588(6)	0.7179(3)	2.67
S2	0.3342(2)	0.43068(6)	0.2593(3)	2.61
C3	0.0437(7)	0.4610(2)	0.4947(9)	2.25
C4	0.1025(8)	0.3100(3)	0.5786(10)	2.78
C5	0.3106(8)	0.3296(3)	0.3683(10)	2.72
C6	0.2174(10)	0.1759(3)	0.4754(13)	4.26
C7	0.4914(10)	0.2006(3)	0.4192(13)	4.31
O8	0.0561(7)	0.2339(2)	0.6815(9)	3.78
O9	0.5018(6)	0.2780(2)	0.2376(9)	3.60
O10	0.462(2)	-0.0067(15)	0.047(2)	8.85
O11	0.8823(16)	0.0169(9)	-0.0083(18)	10.02
Br12	0.6884(16)	0.0198(11)	-0.0538(18)	12.52
Br13	0.7731(15)	0.0260(10)	-0.0730(17)	10.52

The populations of Br12 and Br13 equal 1/8, while those of O10 and O11 are 1/4 and 1/2, respectively. Equivalent isotropic thermal parameters are defined as

$$B_{eq} = (8\pi^2/3)\sum_{i=1}^{3} U_{ii}.$$

were detected by the measurements on an imaging plate. The crystal density determined by floating method in a mixture of carbontetrachloride and 1,2-dibromoethane was 1.80, which is in good agreement with the calculated value (1.81). A total of 1911 reflections were collected by $2\theta-\omega$ scans up to 2θ = 55°. The structure was solved by direct method using SHELXS-86,[19] and were refined by full-matrix least squares method (SHELX-76).[19] Atomic parameters of the non-hydrogen atoms were refined by adopting anisotropic temperature factors for the donor molecule, and isotropic ones for water and bromide. In the refinement of donor molecules, the differential Fourier map presented the counter components, which were distributed as an infinite chain of peaks along the *a* axis. The strongest peaks were assumed to be bromide anions, and the remainder peaks to be water molecules. Since the bromide anions and water molecules are disordered, their occupation factors were smaller than unity. Table I lists the positional and equivalent (or isotropic) thermal parameters. 1416 unique reflections with $Fo \geq 2\sigma(Fo)$ were used for the refinement of 98 variables. The final R and R_w values were 0.070 and 0.080, respectively, by using the weighting scheme, $w = 2.0397/(\sigma^2(Fo) + 0.001267Fo^2)$.

Tight-binding band calculations were based on extended Hückel method, employing the same parameters as that described elsewhere.[5] The transfer integrals (t) are assumed to be proportional to the corresponding overlap integrals by a factor of −10 eV.

D.C. conductivities were measured on a standard four-probe technique. Gold wires were attached by gold paint on a single crystal or on a conducting surface of the film, the opposite side of which was insulating. Thermoelectric powers were measured on the same technique described in Ref.20. Optical measurements, for infrared (IR) regions (400–4000 cm^{-1}) were carried out with Perkin-Elmer 1600 Series FTIR, and for near-infrared, visible and ultraviolet (UV-vis-nearIR) regions on SHIMADZU UV-3100 Spectrometer. UV-Vis-nearIR spectra of the films were measured using the incident light perpendicular or oblique (~30°) to each film.

RESULTS AND DISCUSSION

Crystal Structure of $(BEDO\text{-}TTF)_2Br(H_2O)_3$ (3)

The crystal is elongated along the c direction developing the (010) plane. Since the obtained cell includes only half of the formula unit, the structural analysis assumed the averaged packing of Br^- anion and water molecules. The donor molecule lies on an inversion center, and shows planar geometry except for the terminal ethylene groups of the eclipsed conformation. Each of its bond distance (Table II) agrees with corresponding one in $(BEDO\text{-}TTF^{+0.5})_4SQA^{2-}(H_2O)_6$ (SQA^{2-} = squarate)[5] within an experimental error.

The donor molecules form layers along the ac planes (Figure 1a, b) with c as the stacking direction. The stacking axis tilts by 60.6° to the molecular plane and by 89.0° to the central C=C bond, indicating

TABLE II Bond Distances (Å) for the donor molecule in $(BEDO-TTF)_2Br(H_2O)_3$ (3).

S1 - C3	1.743(4)	C4 - C5	1.348(6)	C6 - O8	1.449(6)
S1 - C4	1.734(4)	C4 - O8	1.357(5)	C7 - O9	1.466(6)
S2 - C3	1.746(4)	C5 - O9	1.346(5)	C3 - C3	1.357(8)
S2 - C5	1.744(4)	C6 - C7	1.534(7)		

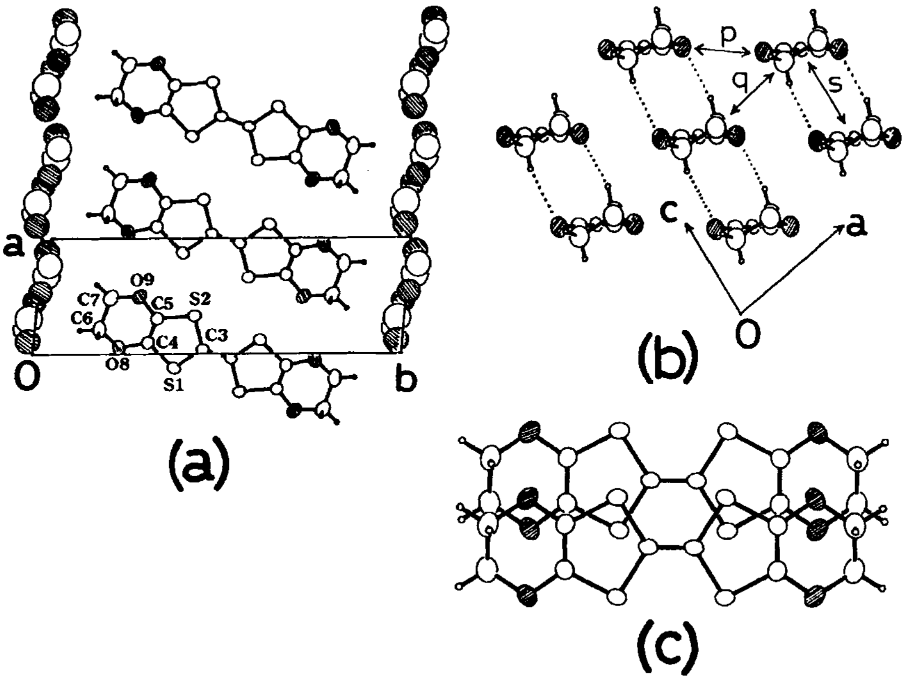

FIGURE 1 $(BEDO-TTF)_2Br(H_2O)_3$ (3). (a) Crystal structure projected along the *c* axis. Oxygen atoms are shaded. (b) Donor packing pattern with scheme of the intermolecular overlap integrals (*s*, *p*, *q*). Short C–H··O contacts are shown by dotted lines. (c) Stacking motif of the donor molecules viewed on the molecule.

the slipped stacking only along the transverse molecular axis (Figure 1c). The donor stack shows the intermolecular separation of 3.50 Å and short intermolecular C–H··O distances (< 2.72 Å, dotted lines in

Figure 1b), but no S··S and S··O contacts shorter than the van der Waals radii (vdW) sums.[21] Each donor molecule is coplanarly linked by three S··S (3.40–3.49 Å) and two S··O (3.27–3.28 Å) atomic contacts with the neighboring ones along the *a*–*c* directions. The long molecular axes are approximately perpendicular to the layer. All the above characteristics and the overall intralayer array are completely the same as the corresponding ones in the $(BEDO\text{–}TTF)_{2.4}I_3$ salt. Therefore, according to our previous classification,[5] this salt is regarded as the I_3 type, which is the most typical packing type as a result of the strong self–aggregation of the molecules in the metallic BEDO–TTF complexes.[5]

The water molecules and Br^- ions are disordered and distributed along the *a* axis. The Br^- anions are connected with the donor molecules by a number of C–H··Br contacts of the short distance (2.73–3.10 Å).

Band Electronic Structure of $(BEDO\text{–}TTF)_2Br(H_2O)_3$ (3)

The intermolecular overlap integrals are large along the side–by–side ($p = 14.6\times10^{-3}$) and oblique directions ($q = -13.4\times10^{-3}$), compared with those for stacking direction ($s = 5.6\times10^{-3}$) (for the labeling of interactions, see Figure 1b). These overlap integrals are very close to the corresponding value in $(BEDO\text{–}TTF)_{2.4}I_3$ (1),[5] reflecting the

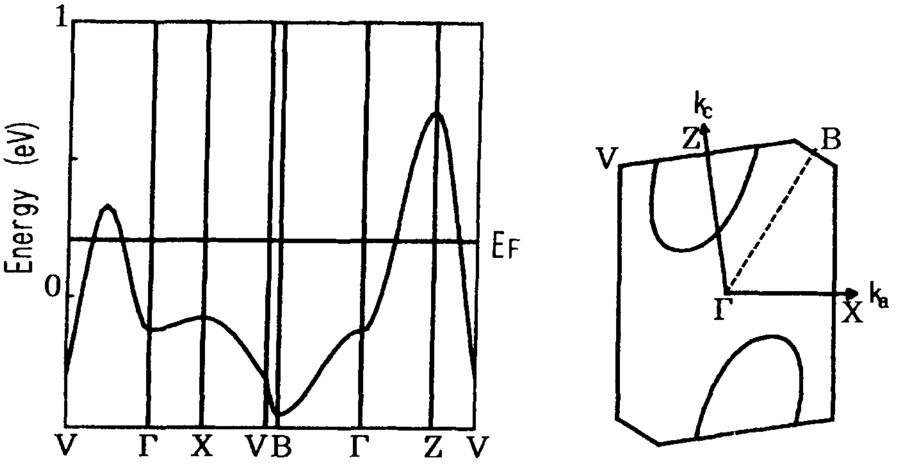

FIGURE 2 Calculated band structure (a) and Fermi surface (b) of $(BEDO\text{–}TTF)_2Br(H_2O)_3$ (3).

isostructural packing of donor molecules. Tight-binding band calculations on 1 and 3 gave similar ellipse-like closed (2D) Fermi surfaces, the areas of which are slightly different from each other (21 % and 25 % of the area of the first Brillioun zone, respectively) due to different degree of CT (+0.42 and +0.50, respectively) (see Figure 2 for the complex 3).

Conductivity

The single crystals of $(BEDO\text{-}TTF)_{2.4}I_3$ (1) and $(BEDO\text{-}TTF)_2Br(H_2O)_3$ (3) show low resistivity at room temperature (3×10^{-2} (//*b*) and 1×10^{-2} $\Omega \cdot$cm (//*c*), respectively). Both are metallic down to the lowest temperature measured (1.3 and 4 K, respectively, Figure 3a).

The PC film of (BEDO-TTF)-iodide remains metallic down to 17 K with a poorer conductivity enhancement factor (2.9) than that of a single crystal of 1 (105). The resistance of the PC film of (BEDO-TTF)-bromide decreases by a factor of 2.1 down to 65 K, below which the resistance gradually increased though it was still smaller than the room temperature value even at 4 K. These facts clearly show that the electron conduction in the films is governed by the continuous network of the metallic crystallites.

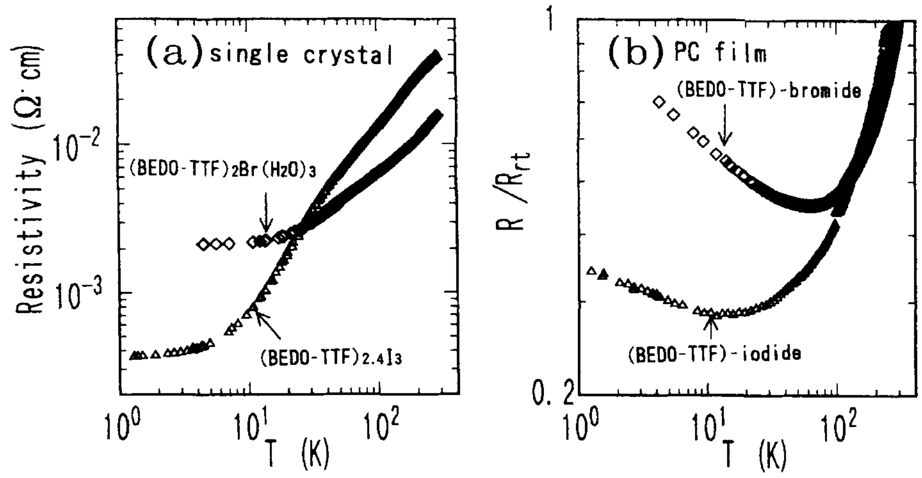

FIGURE 3 (a) Temperature dependent resistivity on single crystals of $(BEDO\text{-}TTF)_{2.4}I_3$ (1, triangles) and $(BEDO\text{-}TTF)_2Br(H_2O)_3$ (3, squares). (b) Temperature dependent resistance for the reticulate-doped PC films of (BEDO-TTF)-iodide (triangles) and of (BEDO-TTF)-bromide (squares).

It should be noted that the reticulate-doped polymers based on TTF-TCNQ lose the metallic nature around 230 K, well above the intrinsic metal-insulator transition temperature of 54 K in bulk crystal.[22] The degraded metallic property was explained by the destruction of crystalline network in the film owing to the presence of defects,[22] since the carrier transport in 1D system is very susceptible to disorders.[23] On the other hand, the composites of BEDO-TTF complexes retain metallic down to much lower temperatures than the above case. Such the improvement is attributed to the nature peculiar to the BEDO-TTF molecule: the molecules construct the self-assembled 2D conduction layer rather easily so as to stabilize the metallic state down to low temperatures, even in the complexes of non-stoichiometric and/or the severely disordered counter molecules.[5]

Thermoelectric Power

For $(BEDO\text{-}TTF)_{2.4}I_3$ (1), the temperature dependent in-plane thermoelectric power, which was reported by T. Suzuki *et al.*,[24] is represented by the broken (//*a*) and dotted curves (//*b*) in Figure 4a. At room temperature, the thermoelectric power (S) was found to

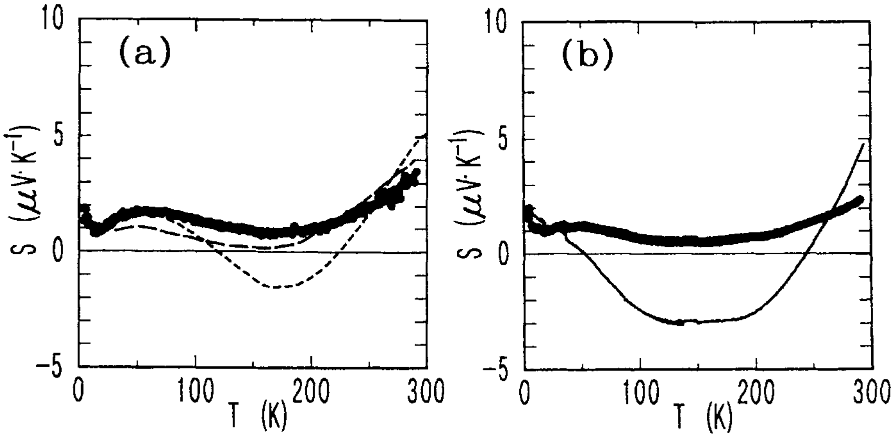

FIGURE 4 Thermoelectric power. (a) On a single crystal for $(BEDO\text{-}TTF)_{2.4}I_3$ (1) (//*a* (interstack) direction, broken curve) and //*b* (stacking) direction, dotted curve), taken from Ref. 24), and on a reticulate-doped film of (BEDO-TTF)-iodide (thick curve). (b) On a single crystal for $(BEDO\text{-}TTF)_2Br(H_2O)_3$ (3) (//*c* (stacking) direction, thin curve), and on a reticulate-doped film of (BEDO-TTF)-bromide (thick curve).

be small positive for both directions (4 and 5 μV/K, respectively). The temperature dependence is somewhat complicated; S decreases with lowering temperature down to 170 K, below which it increases above 60 K and then decreases again. Similarly for (BEDO-TTF)$_2$Br(H$_2$O)$_3$ (3), we found the small positive S (5 μV/K) at room temperature and the minimum S around 150 K as shown by a thin line in Figure 4b.

For both crystals, the positive S at room temperature is consistent with the hole-like character of the calculated Fermi surfaces of 1 and 3. The Boltzmann equation[25] represents the thermoelectric power tensor (S) of metals as

$$S_{ij} = (1/eT)\sum_{k=1}^{3}(L_0{}^{-1})_{ik}(L_1)_{kj}$$

$$(L_0)_{ij} = e^2\int(dk/4\pi^3)(-\partial f^0/\partial\varepsilon)\,\tau\, v_i(\mathbf{k})\, v_j(\mathbf{k})$$

$$(L_1)_{ij} = e^2\int(dk/4\pi^3)(-\partial f^0/\partial\varepsilon)\,\tau\, v_i(\mathbf{k})\, v_j(\mathbf{k})(\varepsilon(\mathbf{k})-\mu)$$

where $(L_0)_{ij}$ and $(L_1)_{ij}$ are tensors, f^0 is the Fermi distribution function, τ is the relaxation time of the carriers, and μ is the chemical potential. The velocity $v = (\partial\varepsilon(\mathbf{k})/\partial\mathbf{k})/\hbar$ at wave vector $\mathbf{k}$ was obtained from the 2D tight-binding band structures as

$$\varepsilon(\mathbf{k}) = 2t_q\cos(\mathbf{k}\cdot\mathrm{a}) + 2t_p\cos[\mathbf{k}\cdot(\mathrm{a}-\mathrm{b})] + 2t_s\cos(\mathbf{k}\cdot\mathrm{b})$$

for the salt 1, and

$$\varepsilon(\mathbf{k}) = 2t_q\cos(\mathbf{k}\cdot\mathrm{a}) + 2t_p\cos[\mathbf{k}\cdot(\mathrm{a}-\mathrm{c})] + 2t_s\cos(\mathbf{k}\cdot\mathrm{c})$$

for the salt 3. The numerical calculation based on the above relations gave the small positive S at room temperature (12 μV/K (//a), 13 μV/K (//b) for 1, and 8 μV/K (//c) for 3), somewhat higher than the experimental values. It should be noted that the small anisotropy in the calculated in-plane S of the both salts is in agreement with the observation for the salt 1. The calculated S is simply proportional to the temperature, and hence, it alone cannot elucidate the minimum peak in S. The complicated temperature dependence may be originated by the scattering mechanism, which has been proposed for the 2D β-(BEDT-TTF)$_2$I$_3$ having a similar ellipse-like Fermi surface.[26]

The PC films of both (BEDO-TTF)-iodide and (BEDO-TTF)-bromide also exhibit the small positive S at room temperature (+3.5 and +2 μV/K, respectively). The room temperature values and the temperature dependence of the *S* (bold lines in Figure 4) are quite resembling to the results on the correspondent single crystals. The above results again show that the transport properties in both polymer composites reflect those of the corresponding metallic BEDO–TTF crystallites.

Optical Absorption Spectra of BEDO–TTF radical salts

Figure 5 shows the optical absorption spectra of $(BEDO\text{–}TTF)_{2.4}I_3$ (1), $(BEDO\text{–}TTF)I_3$ (2), and $(BEDO\text{–}TTF)_2Br(H_2O)_3$ (3) as well as the neutral BEDO–TTF and $[(n\text{–}C_4H_9)_4N]I_3$ on the KBr disk. Based on our previous assignments,[5,17] three kinds of low–lying bands are labeled by A, B, and C. The A bands lying around 2×10^3 cm^{-1} observed for 1 and 3 arise from the CT process among the partially–charged BEDO–TTF molecules. On the other hand for the complex 2, the CT process between the fully–ionized BEDO–TTF$^+$ molecules gives rise to two B

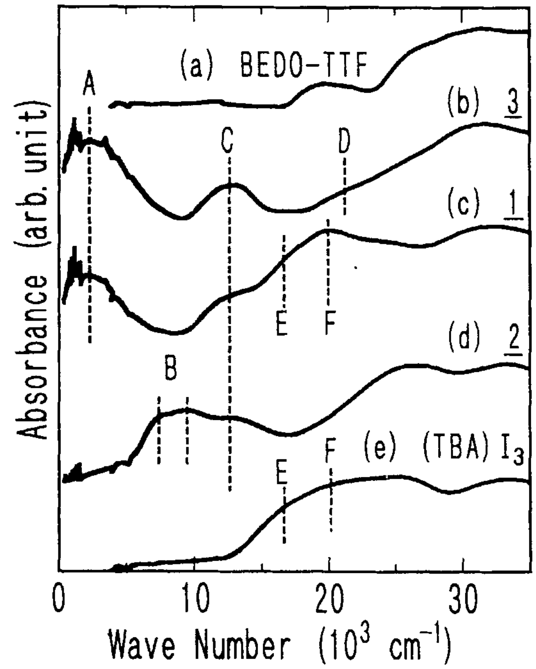

FIGURE 5 Optical absorption spectra of (a) neutral BEDO–TTF, (b) $(BEDO\text{–}TTF)_2Br(H_2O)_3$ (3), (c) $(BEDO\text{–}TTF)_{2.4}I_3$ (1), (d) $(BEDO\text{–}TTF)I_3$ (2), and (e) $[(n\text{–}C_4H_9)_4N]I_3$ on KBr pellets.

bands (intra- and interdimer CT) at higher energy [(8–9)x10^3 cm^{-1}]. The C bands, which are commonly seen around 13x10^3 cm^{-1} for 1–3, are assigned to the intramolecular excitation from the second highest occupied molecular orbital (second HOMO, b_{3g}) to HOMO (b_{1u}) of the BEDO–TTF molecule.

The complex 3 shows weak shoulders around 21x10^3 (band D) and 25x10^3 cm^{-1}, and a peak at 31x10^3 cm^{-1}. Since Br^- ion and H_2O molecule do not absorb the light of this energy region, these bands are unambiguously related to the electronic transition of BEDO–TTF molecules. The weak band D, which is also observed as the lowest electronic band of neutral BEDO–TTF, is attributed to the excitation from HOMO to LUMO.

The complex 1 shows two additional intense bands around (15–20)x10^3 cm^{-1} (bands E and F), which hide the band D. A comparison with the spectra of $[(n\text{-}C_4H_9)_4N]I_3$ indicates that these bands correspond to the lowest intramolecular transitions of I_3^- ion.[27] On the other hand, these two bands cannot be seen for the complex 2, which also contains the I_3^- ions in the crystal.[17] The bands E and F are assigned to the singlet–triplet transitions of the I_3^- ion.[27] They are almost absent in the solution spectra, but increase their intensity particularly with lowering symmetry of the ion. The different appearances of these bands in 1 and 2 seem to be originated from the difference in the symmetry of I_3^-: the ions are located on centers of inversion in 2, whereas the symmetry-lowering is expected in 1 by the modulation from incommensurate donor sublattices.[28]

Optical Absorption Spectra of Reticulate-Doped PC Films

Figure 6 shows the absorption spectra of the PC film of (BEDO–TTF)-iodide and (BEDO–TTF)-bromide. Both of them reveal an absorption below 4x10^3 cm^{-1}, which can be assigned to the band A. The appearance of this band clearly indicates the self-aggregated state of the partially oxidized BEDO–TTF molecules, and corresponds to the metallic character of these films. The infrared region is dominated by rather intense vibrational bands of polycarbonate, which prevented characterizing the vibrational bands from BEDO–TTF in the polymers. The band B is absent for both films, indicating the absence of $(BEDO\text{–}TTF^+)_2$ dimers. The band B was observed around 10x10^3 cm^{-1}

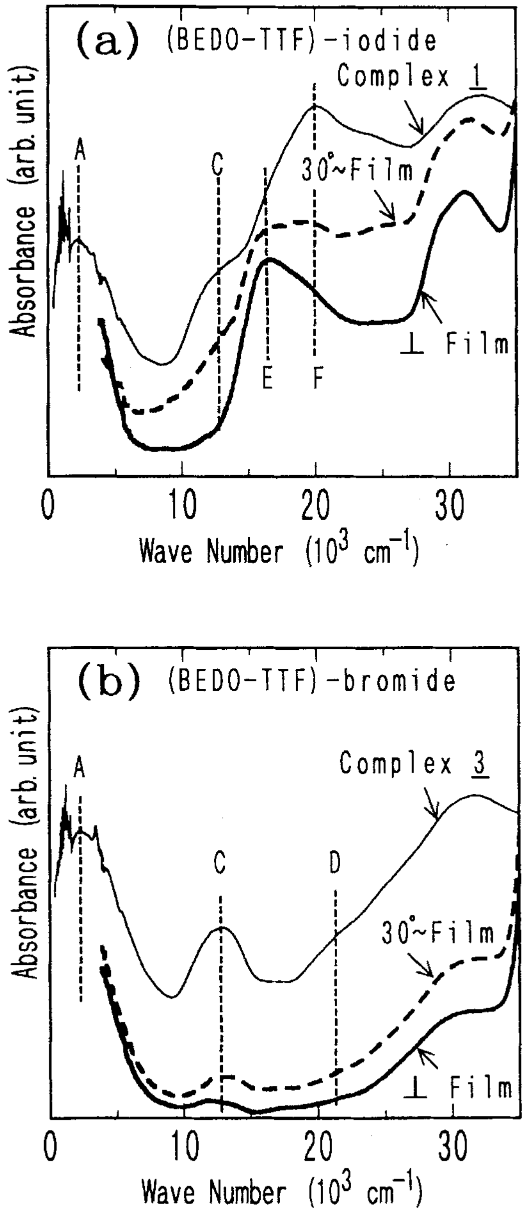

FIGURE 6 Optical absorption spectra of the PC films of (BEDO-TTF)-iodide (a), and of (BEDO-TTF)-bromide. Thick solid and dotted curves represent the absorptions against the perpendicular and oblique (~30°) incident light to each film, respectively. Absorption spectra of the $(BEDO-TTF)_{2.4}I_3$ (1) and $(BEDO-TTF)_2Br(H_2O)_3$ (3) are shown by thin lines.

only for the film with prolonged doping time ($\geq$ 5 min).

Compared with the spectra of (BEDO–TTF)$_{2.4}$I$_3$ (1) and (BEDO–TTF)$_2$Br(H$_2$O)$_3$ (3), the band C is only observed as a very weak peak or a shoulder at around 12x10^3 cm^{-1} in the films. In the case of the film of (BEDO–TTF)-iodide, this band almost disappears against the perpendicular incident light (thick solid curve in Figure 6a), while an absorption appeared around 12x10^3 cm^{-1} against the oblique light (dotted curve in Figure 6a). Similarly for the film of (BEDO–TTF)-bromide, the band C becomes distinct with tilting the film (Figure 6b). These anisotropic optical properties strongly indicate that the ionized BEDO–TTF molecules are well oriented in the films. Since the intramolecular transition C is polarized along the longest axis of the BEDO–TTF molecule, this molecular axis should be almost perpendicular to the film surface as schematized in Figure 7.

Whereas only one weak shoulder D is found in the region (15–22) x10^3 cm^{-1} for the film of (BEDO–TTF)-bromide, the film of (BEDO–TTF)-iodide exhibits intense bands E (16x10^3 cm^{-1}) and F (20x10^3 cm^{-1}), which are related to absorptions of the I$_3^-$ ions. The relative intensities of the E and F bands vary with the film orientation, which indicates the orientational ordering of the I$_3^-$ ion in the film.

The intense bands around 30x10^3 cm^{-1} are observable not only for both films of (BEDO–TTF)-halide salts but also for the film of molecularly dispersed neutral BEDO–TTF. Therefore, these bands are attributed to the absorptions of the unreacted dispersed neutral BEDO–TTF, which is responsible for the insulating nature of the reverse film surfaces of the metallic composites.

Molecular orientation in films

Both (BEDO–TTF)$_{2.4}$I$_3$ (1) and (BEDO–TTF)$_2$Br(H$_2$O)$_3$ (3) crystals contain 2D donor layers, which are approximately perpendicular to the long molecular axis of BEDO–TTF. In addition, both crystals grow with the developed planes parallel to the conducting 2D layers. Therefore, the above discussed molecular orientation means that these metallic crystals grow parallel to the film plane, as shown in Figure 7. Also the 2D donor layer is parallel to the film plane, and thus it is advantageous for the in-plane electron conduction. This crystal orientation is supported for the film of (BEDO–TTF)-iodide by the recent scanning electron microscopy, preliminary X-ray diffraction, and atomic force microscopy.[13,29] Although the actual crystallization process is not well understood at present, a concentration gradient of the complexes, if exists along the film plane normal, seems to orient the crystallites, during exposing the film to the solvent/halogen vapor.

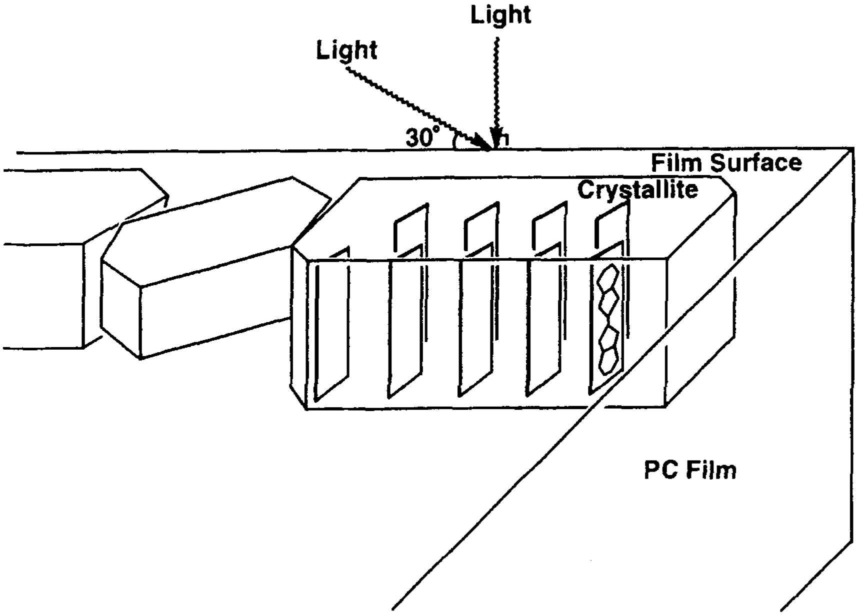

FIGURE 7 Schematic drawing of molecular orientation in reticulate-doped films. Hexagonal plates represent the metallic crystallites, for one of which only one donor layer is illustrated as an assembly of rectangular plates of the donor molecule. In one of the rectangular plates, the molecular shape of BEDO-TTF is drawn.

It should be also noted that the molecular orientation plays an important role for high transparency, particularly for the film of (BEDO-TTF)-bromide. It is highly transparent around the visible region [absorbance of 0.11-0.23 for (10-26)x10^3 cm^{-1}] as shown in Figure 6b, partly due to no absorptions of the visible light by the counter components, unlike the film of (BEDO-TTF)-iodide. Only donor molecule gives rise to the two intramolecular excitations C and D, both of which are polarized along the long molecular axis. Therefore, it is concluded that the molecular orientation discussed above serves to reduce the absorptions of the films, resulted in the high transparency.

CONCLUSION

The metallic reticulate-doped polymer composites based on BEDO-TTF salts are characterized by transport and optical properties. The crystal structure of $(BEDO\text{-}TTF)_2Br(H_2O)_3$ is also determined. The surfaces of both PC films of (BEDO-TTF)-iodide and (BEDO-TTF)-bromide are metallic down to low temperatures, seemingly due to 2D nature of the electronic structures. Thermoelectric power of the film is very small and dominated by the metallic network of the BEDO-TTF salts. They reveal CT bands characteristic to the self-aggregate state of the partially charged donor molecules in the infrared region. Anisotropic optical absorption spectra indicate that the long axis of donor molecules orients approximately in normal to the film plane. Therefore, the conducting layers lie in parallel to the film, forming effective conducting network. The molecular orientation also suppresses the intramolecular excitations against the perpendicular incident visible light, which is also favorable for the high transparency.

DEDICATION

It is our pleasure to dedicate this paper to Professors Yusei Maruyama and Fumio Ogura on the occasion of their retirement from Institute for Molecular Science and Hiroshima University, respectively.

ACKNOWLEDGEMENT

This work was supported by a Grant-in-aid for Science Research from the Ministry of Education, Science, Sports, and Culture, Japan, a Grant for the Proposal-based Advanced Industrial Technology R&D Program from NEDO, Japan, and a Grant from Toyota Physical and Chemical Research Institute. The authors are also grateful to Ms. A. Nakao in MAC Science Co. Ltd. for the measurement on the imaging plate.

REFERENCES

1. D. O. Cowan, J. A. Fortkort, and R. M. Metzger, In Low-Dimensional Systems and Molecular Electronics, edited by R. M. Metzger, P.

Day, and G. C. Papavassiliou (Plenum Press, New York, 1991), p.1.
2. G. Saito, In Metal-Insulator Transition Revisited, edited by P. P. Edwards, and C. N. R. Rao (Taylor & Francis, London, 1995), p.231.
3. J. M. Williams, J. R. Ferraro, R. J. Thorn, K. D. Carlson, U. Geiser, H. H. Wang, A. M. Kini, and M. -H. Whangbo, Organic Superconductors (including Fullerenes): Synthesis, Structure, Properties, and Theory (Prentice Hall, Englewood Cliffs, NJ, 1992).
4. D. Jerome, and H. J. Schulz, Adv. Phys., 31, 299 (1982).
5. S. Horiuchi, H. Yamochi, G. Saito, K. Sakaguchi, and M. Kusunoki, J. Am. Chem. Soc., 118, 8604 (1996).
6. S. Horiuchi, H. Yamochi, G. Saito, and K. Matsumoto, Synth. Met., in press.
7. H. Yamochi, T. Nakamura, G. Saito, T. Kikuchi, S. Sato, K. Nozawa, M. Kinoshita, T. Sugano, and F. Wudl, Synth. Met., 41-43, 1741 (1991).
8. T. Nakamura, G. Yunome, R. Azumi, M. Tanaka, H. Tachibana, M. Matsumoto, S. Horiuchi, H. Yamochi, and G. Saito, J. Phys. Chem., 98, 1882 (1994).
9. T. Nakamura, H. Isotalo, T. Akutagawa, H. Tachibana, R. Azumi, M. Matsumoto, S. Horiuchi, H. Yamochi, and G. Saito, Mol. Cryst. Liq. Cryst., 284, 235 (1996).
10. K. Ogasawara, T. Ishiguro, S. Horiuchi, H. Yamochi, and G. Saito, Jpn. J. Appl. Phys., 35, L571 (1996).
11. J. K. Jeszka, J. Ulański, and M. Kryszewski, Nature, 289, 390 (1981).
12. A. Tracz, J. K. Jeszka, A. Sroczyńska, J. Ulański, J. Plocharski, H. Yamochi, S. Horiuchi, and G. Saito, Synth. Met., in press.
13. A. Tracz, J. K. Jeszka, A. Sroczynska, S. Schrader, K. Pfeiffer, J. Ulański, M. Kryszewski, Adv. Mater. Opt. Electr., submitted.
14. J. Ulański, and M. Kryszewski, "Reticulate Composites" in Encyclopedia of Advanced Materials, edited by D. Bloor, R. J. Brook, M. C. Flemings, S. Mahajan, and R. W. Cahn (Pergamon, London, 1995) p.2301.
15. E. E. Laukhina, V. A. Merzhanov, S. I. Pesotskii, A. G. Khomenko, E. B. Yagubskii, J. Ulański, M. Kryzewski, and J. K. Jeszka, Synth. Met., 70, 797 (1995).
16. F. Wudl, H. Yamochi, T. Suzuki, H. Isotalo, C. Fite, H. Kasmai, K. Liou, and G. Srdanov, J. Am. Chem. Soc., 112, 2461 (1990).
17. S. Horiuchi, H. Yamochi, G. Saito, and K. Matsumoto, Mol. Cryst. Liq. Cryst., 284, 357 (1996).
18. J. K. Jeszka, and A. Tracz, Polymer Adv. Tech., 3, 139 (1992).
19. G. M. Sheldrick, SHELXS-86 Program for Crystal Structure Determination, and SHELX-76 Program for Crystal Structure Determination, University of Götingen, Federal Republic of Germany.
20. T. Komatsu, H. Sato, T. Nakamura, N. Matsukawa, H. Yamochi, G. Saito, M. Kusunoki, K. Sakaguchi, and S. Kagoshima, Bull. Chem. Soc. Jpn., 68, 2233 (1995).
21. The vdW employed in this paper are as follows; C 1.70 Å, H 1.20 Å, O 1.52 Å, S 1.80 Å. A. Bondi, J. Phys. Chem., 68, 441 (1964).
22. J. Ulański, Synth. Met., 39, 25 (1990).
23. L. Zuppiroli, M. Przybylski, and W. Pukacki, J. Physique., 45, 1925 (1984).
24. T. Suzuki, H. Yamochi, H. Isotalo, C. Fite, H. Kasmai, K. Liou, G.

Srdanov, F. Wudl, P. Coppens, K. Maly, and A. Frost-Jensen, Synth. Met., 41-43, 2225 (1991).

25. N. W. Ashcroft, N. D. Mermin, Solid State Physics, (Saunders College, Philadelphia, 1976), eqs(13.46) and (13.61).
26. K. Mortensen, J. M. Williams, and H. H. Wang; Solid State Commun., 56, 105 (1985).
27. W. Gabes, and D. J. Stufkens, Spectrochim. Acta, 30A, 1835 (1974).
28. I. Cisarova, K. Maly, X. Bu, A. Frost-Jensen, P. Sommer-Larsen, and P. Coppens, Chem. Mater., 3, 647 (1991).
29. A. Tracz *et al.*, to be published.